INSTITUT DE FRANCE
Académie des sciences

Comptes Rendus

Mécanique

Nourhaine Yousfi, Bacem Zghal, Ali Akrout, Lassaad Walha
and Mohamed Haddar

Estimation of the damping model of a spur gear pair system including a time-varying loading

Volume 350 (2022), p. 255-267

Published online: 16 June 2022

https://doi.org/10.5802/crmeca.104

CENTRE MERSENNE

Les Comptes Rendus. Mécanique *sont membres du*
Centre Mersenne pour l'édition scientifique ouverte
www.centre-mersenne.org
e-ISSN : 1873-7234

Comptes Rendus
Mécanique
2022, 350, p. 255-267
https://doi.org/10.5802/crmeca.104

Historical article / *Article historique*

Estimation of the damping model of a spur gear pair system including a time-varying loading

Nourhaine Yousfi[*, a, b], **Bacem Zghal**[a], **Ali Akrout**[a, b], **Lassaad Walha**[*, a] **and Mohamed Haddar**[a]

[a] Mechanics, Modelling and Production Research Laboratory (LA2MP), Engineering National School of Sfax, University of Sfax, Tunisia

[b] Engineering National School of Tunis, University of Tunis El-Manar, Tunisia

E-mails: nourhainegem@gmail.com (N. Yousfi), bacem.zghal@isgis.rnu.tn (B. Zghal), ali_akrout2005@yahoo.fr (A. Akrout), walhalassaad@yahoo.fr (L. Walha), mohamed.haddar@enis.rnu.tn (M. Haddar)

Abstract. The integral method was used in a previous research to identify the damping model but this technique has some limitations in estimating the damping model in a gear system including time-varying loading conditions. To overcome these limitations, the integral method is reformulated in this research to identify the damping model on spur gear pair system including variable loading. The motion equations presented in terms of integrals, including time-varying loading conditions, are solved by linear least squares method to characterise the constant piecewise model. Continuous wavelet transform method is used to validate the constant damping model. The new methodology is tested with a signal obtained from numerical simulation.

Keywords. Time-varying loading conditions, Integral method, Wavelet demodulation, Damping model, Gear system.

Manuscript received 29th October 2021, revised 15th February 2022, accepted 28th February 2022.

1. Introduction

Several research have focused on gear systems in stationary settings with constant speed and load. The presence of time-varying loading conditions in a gear system, on the other hand, will significantly alter its vibration levels.

Concerning studies devoted to variable loading conditions, Randall *et al.* [1] investigated the influence of varying external load on vibration level. Chaari *et al.* [2] studied the influence of

* Corresponding authors.

the loading shape on the vibration characteristics of the transmission. Guangjian *et al.* [3] investigated the influence of the time-varying excitation on the dynamic transmission error (DTE). Rocca *et al.* [4] presented the effect of varying speed on the DTE of a gear system. Hammami *et al.* [5] considered the different loading conditions to show the nonlinear behaviour of the gearbox. Liu *et al.* [6] presented the variation of the damping ratio in gear teeth contacts under lightly loaded hydrodynamic conditions. Rayleigh damping is usually used to model damping on gear systems presented by the mass matrix and stiffness matrix. The current viscous damping model has a number of limitations [7, 8], so an advanced formulation for viscous damping in the time-frequency domain that is dependent on dominant frequency is developed [9]. However, practically every technique is utilized to find damping on a gear system with a constant load. Studies proved that the damping ratio depends on the operating conditions such as load [10–12]. So, the presence of this variability will complicate the technique of identification of the damping model. The first step to overcome this difficulty is to develop a method to estimate damping model under varying loading conditions.

Yousfi *et al.* [13] proposed a model-based technique to evaluate damping model of a one stage spur gear system including a constant load. He presented a constant piecewise model of damping which is related to the evolution of the transmission error.

This work intends to be an extension of the technique presented in that paper [13] by achieving a time-varying model of damping on gear system including time-varying loading conditions.

In this research, we present the limits of the integral method presented in [13] in identifying damping in the case of time-varying excitation force. Then, we reformulated the algorithm of the integral method presented, to identify the damping model in the gear system with time-varying stiffness and time-varying excitation forces. Finally, a one-stage gear system with mesh stiffness fluctuation and time-varying loading is modeled and a numerical example is used to validate the proposed method.

2. The dynamic modeling

The dynamic model of the gear system is illustrated in Figure 1. It consists of a spur gear pair with radius R_1 and R_2, masses m_1 and m_2, moments of inertia I_1 and I_2. A time-varying loading condition is applied to the gear system. $\Theta_1(t)$ and $\Theta_2(t)$ are the two rotation degrees of freedom.

According to Newton's laws of motion, the differential equations of the gear system are given by

$$\begin{cases} I_1 \dfrac{\mathrm{d}^2\theta_1}{\mathrm{d}t^2} + R_1 c(t)\left(R_1 \dfrac{\mathrm{d}\theta_1}{\mathrm{d}t} - R_2 \dfrac{\mathrm{d}\theta_2}{\mathrm{d}t}\right) + R_1 k(t)(R_1\theta_1 - R_2\theta_2) = T_1(t) \\ I_2 \dfrac{\mathrm{d}^2\theta_2}{\mathrm{d}t^2} - R_2 c(t)\left(R_1 \dfrac{\mathrm{d}\theta_1}{\mathrm{d}t} - R_2 \dfrac{\mathrm{d}\theta_2}{\mathrm{d}t}\right) - R_2 k(t)(R_1\theta_1 - R_2\theta_2) = -T_1(t), \end{cases} \tag{1}$$

where $c(t)(R_1(\mathrm{d}\theta_1/\mathrm{d}t) - R_2(\mathrm{d}\theta_2/\mathrm{d}t))$ is the damping force, $k(t)(R_1\theta_1 - R_2\theta_2)$ is the mesh elastic force and $k(t)$ is the mesh stiffness fluctuation, $F(t)$ is the time-varying excitation force. The variation of the meshing stiffness is presented using the square waveform in the following function [14]

$$k(t) = \left\{ \begin{array}{l} K_{\max} \ldots \text{for } 0 < t < (\varepsilon_\alpha - 1)T_e \\ K_{\min} \ldots \text{for } (\varepsilon_\alpha - 1)T_e < t < T_e \end{array} \right\}, \tag{2}$$

where T_e is the meshing period, ε_α is the contact ratio and $K_{\max}$ and $K_{\min}$ are the extremum values of stiffness.

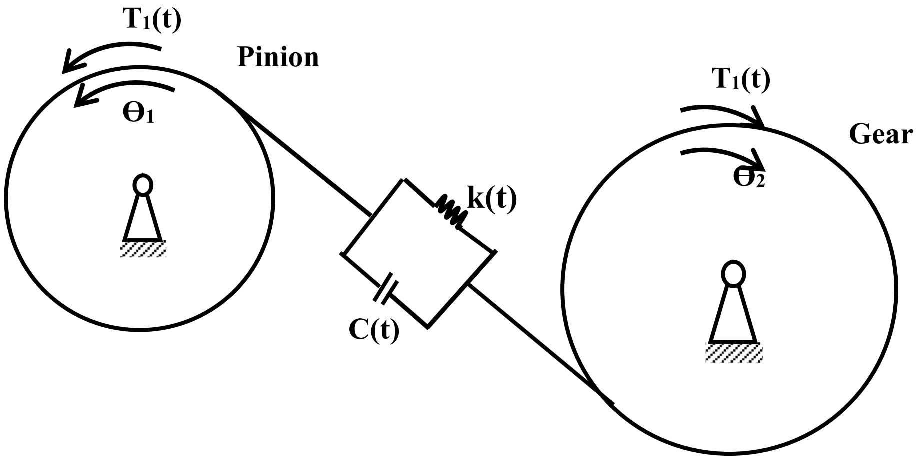

Figure 1. The dynamic model of spur gear-pair system.

Equation (1) can be presented in the following equation by introducing the equivalent mass M_e and the DTE of the gear system, namely, $y = R_1\theta_1 - R_2\theta_2$

$$M_e \frac{\mathrm{d}^2 y}{\mathrm{d}t^2} + c(t)\frac{\mathrm{d}y}{\mathrm{d}t} + k(t)\,y = M_e\left(\frac{R_1}{I_1} + \frac{R_2}{I_2}\right) T_1(t)$$
$$\text{where: } M_e = \frac{I_1 I_2}{I_1 R_2^2 + I_2 R_1^2}. \tag{3}$$

The equation of motion presented in (3) can be given in the non-dimensional form as

$$\frac{\mathrm{d}^2 y}{\mathrm{d}t^2} + C(t)\frac{\mathrm{d}y}{\mathrm{d}t} + K(t)\,y = F(t)$$
$$\text{where: } F(t) = \frac{T_1(t)R_1}{I_1} + \frac{T_1(t)R_2}{I_2}. \tag{4}$$

$F(t)$ represents the time-varying external excitation. The variation of the external load increases the difficulty of identifying damping. That is why the current integral method presented in [13] cannot be used to estimate damping model in the case of a varying load.

In this paper, the damping is estimated using a new formulation of the integral method to obtain the most suitable prediction of the dynamic response.

3. New formulation of the integral method

The dynamic equilibrium equation of a single-degree-of-freedom (SDOF) system with time-varying rigidity, time-varying excitation force and unknown model of damping $C(t)$ can be expressed by (4), where $y(t)$ is the observed response (m) from the system, $F(t)$ is the time-varying force (N), $K(t)$ is the time-varying rigidity (N/m), and $C(t)$ the unknown damping. In each defined time interval ΔT, the damping is considered as a piecewise constant model as is presented in the following equation

$$\begin{aligned} C(t) &= C_0, \quad T_0 < t < T_1 \\ C(t) &= C_1, \quad T_1 < t < T_2 \\ &\vdots \\ C(t) &= C_{n-1}, \quad T_{n-1} < t < T_n. \end{aligned} \tag{5}$$

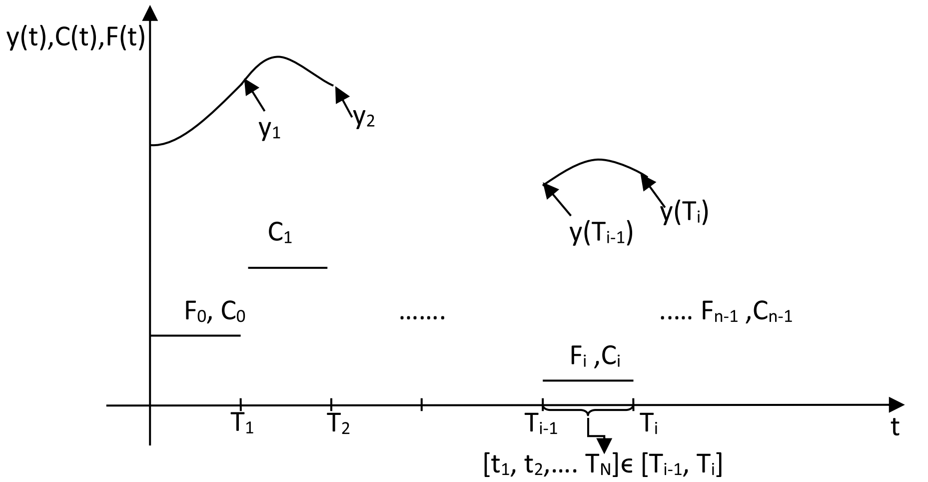

Figure 2. Piecewise model of the observed response and damping $C(t)$.

The identification is based on the sampled observed data presented in Figure 2. The observed data can be a simulated data or a raw testing data.

$\Delta T = T_{i+1} - T_i; i = 0,\ldots,n-1$ presents the defined time interval and n is the number of damping values at $[0, t]$.

The idea of this method is to transform the observed data by the integral operator. Then the values of damping can be directly obtained by using the linear least square method.

The integral method is presented by an algorithm created by Matlab and the integrals in the following equations are calculated using the trapezium method. This methodology has been used in the identification of damping in an electromechanical system [15] with constant stiffness and constant force. In this work, a new formulation is created to estimate the damping model in gear system with time-varying stiffness and time-varying load.

To identify the values of $C(t)$ from the measured data of the system, Equation (4) is double integrated from T_{i-1} to $t \in [T_{i-1}, T_i]$ yielding

$$y_{\text{model},i}(t) = y_{i-1} + \alpha_{i-1}(t - T_{i-1}) - C_i \int_{T_{i-1}}^{t} y_m \mathrm{d}t - K_i \int_{T_{i-1}}^{t}\int_{T_{i-1}}^{t} y_m \mathrm{d}t\mathrm{d}t + F_i \int_{T_{i-1}}^{t} (t - T_{i-1})\mathrm{d}t \tag{6}$$

where

$$y_{i-1} = y(T_{i-1});\ y'_{i-1} = y'(T_{i-1});\ i = 1,\ldots,n$$

$$\alpha_{i-1} = y'_{i-1} + C_i y_{i-1}.$$

The concept of the integral method based on the choice of N time points $(t_1{}^{(i)},\ldots,t_N{}^{(i)})$ in each segment of $[T_{i-1}, T_i], i = 1,\ldots,n$ gives nN equations with $4n+1$ unknown parameters $\{\mathbf{y_0},\ldots,\mathbf{y_{n-1}},\boldsymbol{\alpha_0},\ldots,\boldsymbol{\alpha_{n-1}},\mathbf{C_0},\ldots,\mathbf{C_{n-1}},\mathbf{K_0},\ldots,\mathbf{K_{n-1}},\mathbf{F_0},\ldots,\mathbf{F_{n-1}}\}$. These parameters can be directly obtained by using the well-known linear least squares method of the measured data to obtain the matrix form

$$\mathbf{Aa} = \mathbf{b} \tag{7}$$

where

$$\mathbf{a} = \{\mathbf{y_0},\ldots,\mathbf{y_{n-1}},\boldsymbol{\alpha_0},\ldots,\boldsymbol{\alpha_{n-1}},\mathbf{C_0},\ldots,\mathbf{C_{n-1}},\mathbf{K_0},\ldots,\mathbf{K_{n-1}},\mathbf{F_0},\ldots,\mathbf{F_{n-1}}\}^{\mathbf{T}} \tag{8}$$

$$\mathbf{A} = [\mathbf{A_1}|\mathbf{A_2}|\mathbf{A_3}] \tag{9}$$

$$\mathbf{A_1} = \begin{bmatrix} \mathbf{l_{N,1}}^{(1)} & \mathbf{O_{N,1}} & \cdots & \mathbf{O_{N,1}} \\ \mathbf{O_{N,1}} & \mathbf{l_{N,1}}^{(2)} & \cdots & \mathbf{O_{N,1}} \\ \vdots & \vdots & \ddots & \vdots \\ \mathbf{O_{N,1}} & \mathbf{O_{N,1}} & \cdots & \mathbf{l_{N,1}}^{(\mathbf{n})} \end{bmatrix}; \quad \mathbf{A_2} = \begin{bmatrix} \mathbf{T_{N,1}}^{(1)} & \mathbf{O_{N,1}} & \cdots & \mathbf{O_{N,1}} \\ \mathbf{O_{N,1}} & \mathbf{T_{N,1}}^{(2)} & \cdots & \mathbf{O_{N,1}} \\ \vdots & \vdots & \ddots & \vdots \\ \mathbf{O_{N,1}} & \mathbf{O_{N,1}} & \cdots & \mathbf{T_{N,1}}^{(\mathbf{n})} \end{bmatrix} \tag{10}$$

$$\mathbf{A_3} = \begin{bmatrix} \mathbf{P_{N,1}}^{(1)} & \mathbf{O_{N,1}} & \cdots & \mathbf{O_{N,1}} & \mathbf{R_{N^*1}}^{(1)} & \mathbf{O_{N,1}} & \cdots & \mathbf{O_{N,1}} & \mathbf{F_{N^*1}}^{(1)} & \mathbf{O_{N,1}} & \cdots & \mathbf{O_{N,1}} \\ \mathbf{O_{N,1}} & \mathbf{P_{N,1}}^{(2)} & \cdots & \mathbf{O_{N,1}} & \mathbf{O_{N^*1}} & \mathbf{R_{N,1}}^{(2)} & \cdots & \mathbf{O_{N,1}} & \mathbf{O_{N^*1}} & \mathbf{F_{N,1}}^{(2)} & \cdots & \mathbf{O_{N,1}} \\ \vdots & \vdots & \ddots & \vdots & \vdots & \vdots & \ddots & \vdots & \vdots & \vdots & \ddots & \vdots \\ \mathbf{O_{N,1}} & \mathbf{O_{N,1}} & \cdots & \mathbf{P_{N,1}}^{(\mathbf{n})} & \mathbf{O_{N^*1}} & \mathbf{O_{N,1}} & \cdots & \mathbf{R_{N,1}}^{(\mathbf{n})} & \mathbf{O_{N^*1}} & \mathbf{O_{N,1}} & \cdots & \mathbf{F_{N,1}}^{(\mathbf{n})} \end{bmatrix} \tag{11}$$

$$\mathbf{F_{N^*1}}^{(\mathbf{i})} = \begin{bmatrix} \mathbf{0.5F(t_1}^{(\mathbf{i})} - \mathbf{T_{i-1})^2} \\ \vdots \\ \mathbf{0.5F(t_N}^{(\mathbf{i})} - \mathbf{T_{i-1})^2} \end{bmatrix} \quad \text{for: } i = 1,\ldots,n \tag{12}$$

$$P_{\mathbf{N^*1}}^{(\mathbf{i})} = \begin{bmatrix} -\int_{\mathbf{T_{i-1}}}^{\mathbf{t_1}^{(\mathbf{i})}} \mathbf{y_m dt} \\ \vdots \\ -\int_{\mathbf{T_{i-1}}}^{\mathbf{t_N}^{(\mathbf{i})}} \mathbf{y_m dt} \end{bmatrix}; \quad \mathbf{T_{N^*1}}^{(\mathbf{i})} = \begin{bmatrix} \mathbf{t_1}^{(\mathbf{i})} - \mathbf{T_{i-1}} \\ \vdots \\ \mathbf{t_N}^{(\mathbf{i})} - \mathbf{T_{i-1}} \end{bmatrix}; \quad \mathbf{R_{N^*1}}^{(\mathbf{i})} = \begin{bmatrix} -\int_{\mathbf{T_{i-1}}}^{\mathbf{t_1}^{(\mathbf{i})}} \int_{\mathbf{T_{i-1}}}^{\mathbf{t}} \mathbf{y_m dtdt} \\ \vdots \\ -\int_{\mathbf{T_{i-1}}}^{\mathbf{t_N}^{(\mathbf{i})}} \int_{\mathbf{T_{i-1}}}^{\mathbf{t}} \mathbf{y_m dtdt} \end{bmatrix}. \tag{13}$$

$\mathbf{l_{N^*1}} =$ Matrix of ones, $\mathbf{O_{N^*1}} =$ Matrix of zeros

$$\mathbf{b} = \begin{bmatrix} \boldsymbol{\beta}_{\mathbf{N,1}}^{(1)} \\ \boldsymbol{\beta}_{\mathbf{N,1}}^{(2)} \\ \boldsymbol{\beta}_{\mathbf{N,1}}^{(3)} \\ \vdots \\ \boldsymbol{\beta}_{\mathbf{N,1}}^{(\mathbf{n})} \end{bmatrix}; \quad \boldsymbol{\beta}_{\mathbf{N,1}}^{(\mathbf{i})} = \begin{bmatrix} \mathbf{y_m(t_1}^{(\mathbf{i})}) \\ \vdots \\ \vdots \\ \mathbf{y_m(t_N}^{(\mathbf{i})}) \end{bmatrix}. \tag{14}$$

The damping $C(t)$ in (5) can be considered as constant at each interval ΔT which is equivalent to applying equality constraints $C_1 = C_2 = \ldots C_{n-1}$. Setting $y_m = y_{\text{observed data}}$ for $t = \{t_1{}^{(i)},\ldots,t_N{}^{(i)}, i = 1,\ldots,N\}$ gives $4+n$ parameters ($\mathbf{y_0}$ $\boldsymbol{\alpha_0}$ $\mathbf{C}$ $\mathbf{K_0}$ $\mathbf{K_1},\ldots,\mathbf{K_{n-1}}$ $\mathrm{F}_0,\ldots,\mathbf{F_{n-1}}$) defined by the matrix equation

$$\mathbf{A_{const}a_{const}} = \mathbf{b_{const}} \tag{15}$$

where

$$\mathbf{A_{const}} = \begin{bmatrix} \mathbf{l_{N,1}}^{(1)} & \mathbf{T_{N,1}}^{(1)} & \mathbf{P_{N,1}}^{(1)} & \mathbf{R_{N,1}}^{(1)}\mathbf{F_{N,1}}^{(1)} \\ \vdots & \vdots & \vdots & \vdots \\ \mathbf{l_{N,1}}^{(\mathbf{n})} & \mathbf{T_{N,1}}^{(\mathbf{n})} & \mathbf{P_{N,1}}^{(\mathbf{n})} & \mathbf{R_{N,1}}^{(\mathbf{n})}\mathbf{F_{N,1}}^{(1)} \end{bmatrix}; \quad \mathbf{a_{const}} = \begin{bmatrix} \mathbf{y0} \\ \boldsymbol{\alpha}\mathbf{0} \\ \mathbf{C} \\ \mathbf{K_0} \\ \mathbf{K_1} \\ \vdots \\ \mathbf{K_n} \\ \mathbf{F_1} \\ \vdots \\ \mathbf{F_n} \end{bmatrix}; \quad \mathbf{b_{const}} = \begin{bmatrix} \boldsymbol{\beta}_{\mathbf{N,1}}^{(1)} \\ \boldsymbol{\beta}_{\mathbf{N,1}}^{(2)} \\ \boldsymbol{\beta}_{\mathbf{N,1}}^{(3)} \\ \vdots \\ \boldsymbol{\beta}_{\mathbf{N,1}}^{(\mathbf{n})} \end{bmatrix}. \tag{16}$$

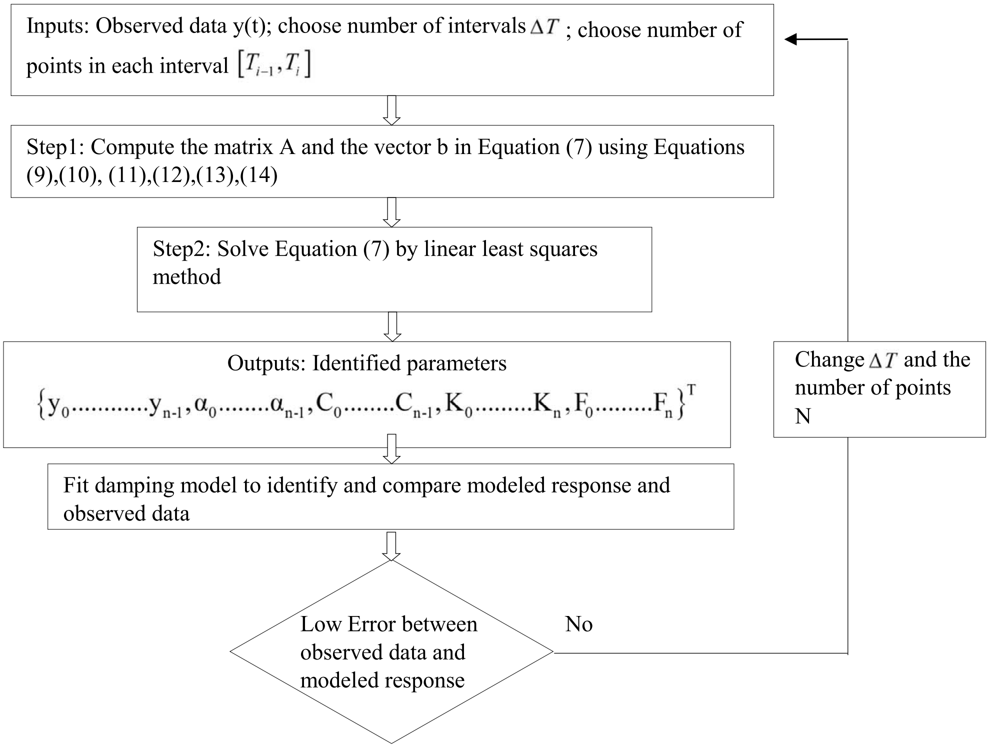

Figure 3. Algorithm for estimation of the damping $C(t)$ in the case of time-varying excitation force.

The methodology of damping identification is presented in Figure 3. It is important to realize that the integral method was used on free damped systems with constant rigidity. In this approach, we considered the time-varying excitation force with time-varying stiffness presented in (4) which required a new formulation compared to [13, 15–17].

In the case of equality constraints, the identified value of damping $C(t)$ in (16) can be validated using wavelet demodulation method (Continuous Wavelet Transform: CWT) which is presented in the following section.

4. Results and discussion

In this study, the performance of the proposed damping extraction methods is validated based on a simulated example. Only the simulated response and the algorithm of the integral method presented in Figure 3 are used to identify the damping model.

The example used to validate the proposed integral method is a spur gear system presented in Section 2 having the parameters as used in [13]. The differential equation of the gear system is given by (4). The free response of the system was simulated using second-order Runge–Kutta procedure with assumed initial conditions as $y(0) = 0$ and $y'(0) = 0$ to obtain the simulated data presented in Figure 5 which corresponds to the transmission error of the spur pair-gear with time-varying mesh stiffness $K(t)$ illustrated in Figure 4(a) and a time-varying loading condition as shown in Figure 4(b).

Integral method is applied to the simulated data presented in Figure 5 to identify the model of damping and to emphasize the effect of the varying load.

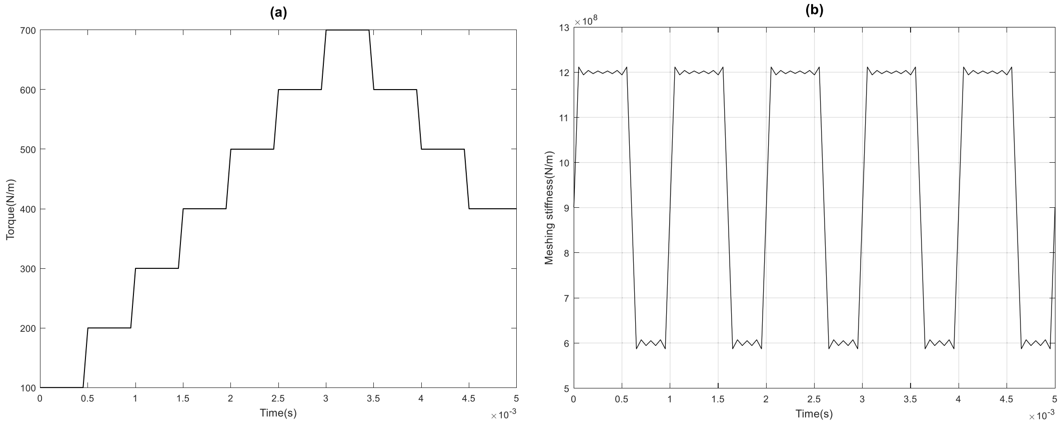

Figure 4. (a) The external variable torque. (b) Time-varying mesh stiffness.

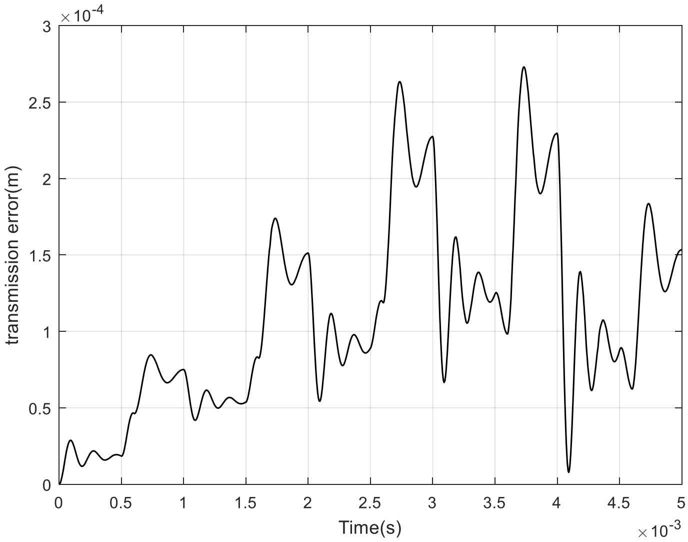

Figure 5. The response of the gear-pair system (DTE).

Table 1. Parameters of spur pair-gear system [13]

	Pinion	Gear
Teeth numbers	20	40
Inertia moments (kg·m^2)	0.00026	0.0045
Base circle (m)	0.05	0.11
Stiffness (N/m)	$K_{\max} = 4 \times 10^8$; $K_{\min} = 2 \times 10^8$	
Module (m)	0.003	
Pressure angle (°)	20	
Contact ratio	1.6	
Teeth width (m)	0.023	
Torque $T_1(t)$ (N·m)	Time-varying torque presented in figure	

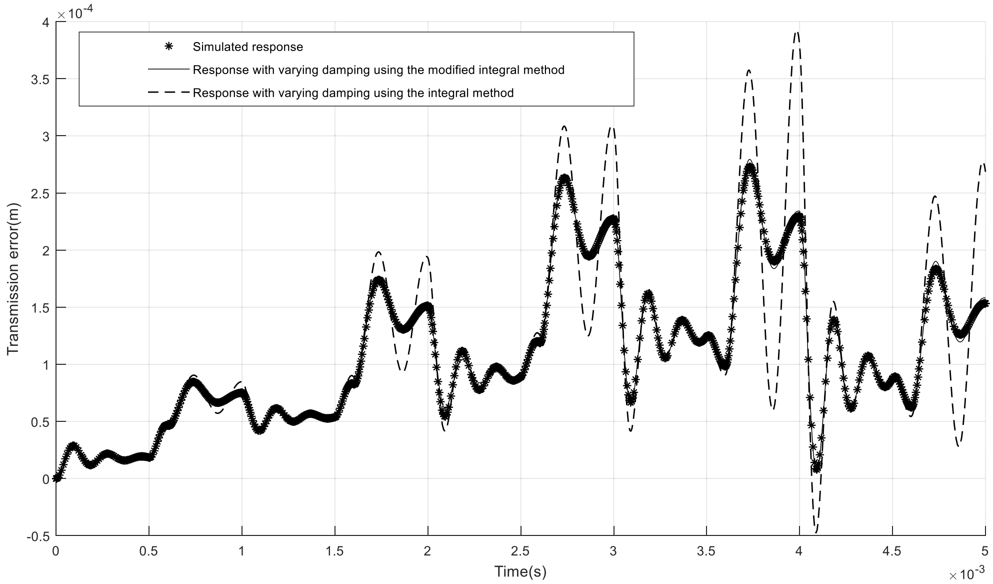

Figure 6. Identified damping modeled response using integral method versus observed response of spur pair-gear system.

4.1. *Limits of the current integral method*

Using the integral method presented in [13] and replacing the estimated damping C in (4) by its expression in (5) gives a second-order system which is transformed quite easily as two coupled equations using the relationships between velocity, position, and acceleration in order to solve it using a Runge–Kutta numerical integration algorithm. The resulting modeled response versus the simulated response is illustrated in Figure 8. There is a big error between the two responses. In addition, the constant damping model obtained using the current integral method does not capture the estimated signal. So, the integral method fails to identify the realistic damping in the system and another representation of the integral must be presented to predict the measured data.

4.2. *Validation of the new formulation of the integral method*

4.2.1. *Constant damping*

In the first step, the unknown damping C in (5) is considered as constant for all time. To identify this parameter, the algorithm of Figure 3 is applied to the simulated data in Figure 6 with time-varying rigidity and time-varying excitation force plotted in Figure 5. Thanks to the new technique, the identified damping C is

$$C = 1.053 \times 10^4 \text{ kg}\cdot\text{s}^{-1}. \tag{17}$$

Replacing C in (4) by its expression in (17) gives a second-order system which is transformed quite easily as two coupled equations using the relationships between velocity, position, and acceleration in order to solve it using a Runge–Kutta numerical integration algorithm. The resulting modeled response versus the simulated response is illustrated in Figure 7. There is an error between the two responses. In addition, the constant damping model does not capture the decrease after 0.000124 s and it underestimates the peak responses.

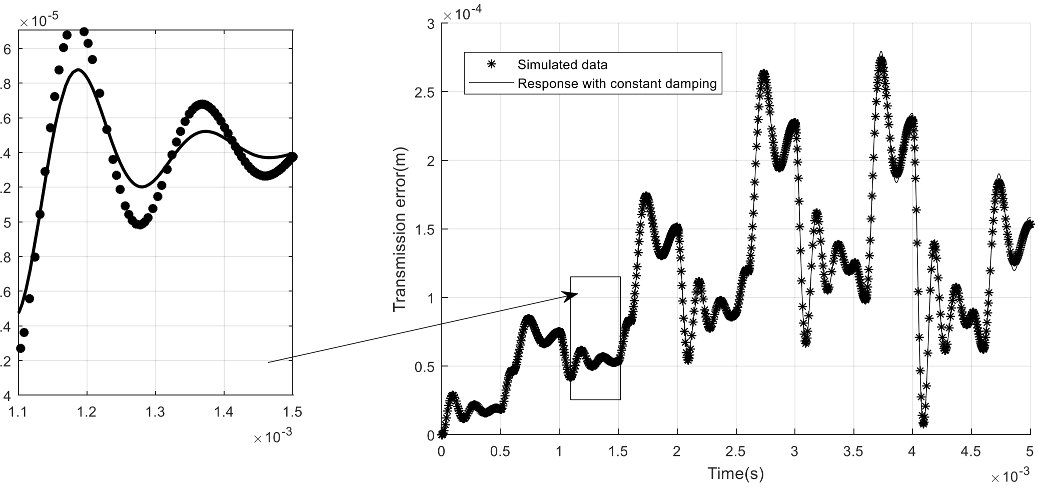

Figure 7. Identified constant damping modeled response versus observed response of spur pair-gear system.

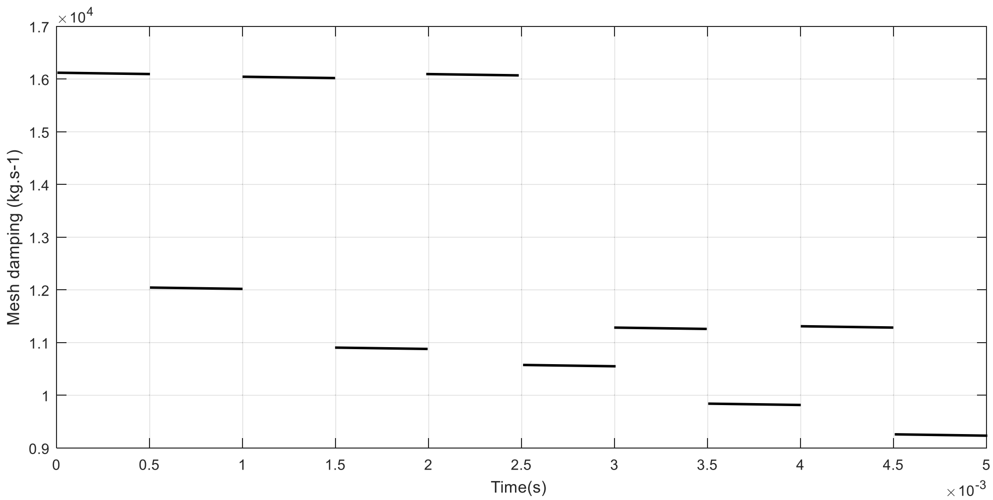

Figure 8. Identified time-varying damping $C(t)$.

It has been concluded that the presence of a time-varying loading condition in a gear system will substantially affect the damping value in each interval. So, the constant damping cannot predict the simulated response and it is essential to find a time-varying model of damping.

4.2.2. *Time-varying damping*

In this section, the unknown damping $C(t)$ varies along time as presented in (5), where $\Delta T = 0.001$ s. The steps presented in Figure 3 are applied to the data in Figure 5 giving a sequence of ten values for $C(t)$ presented in Figure 8. From the obtained results, it can be observed that the mean of the identified ten values of damping is close to the constant damping identified in (17).

The modeled response is presented in Figure 9. It can be observed that compared to the constant damping, the modeled response obtained using the time-varying model of damping

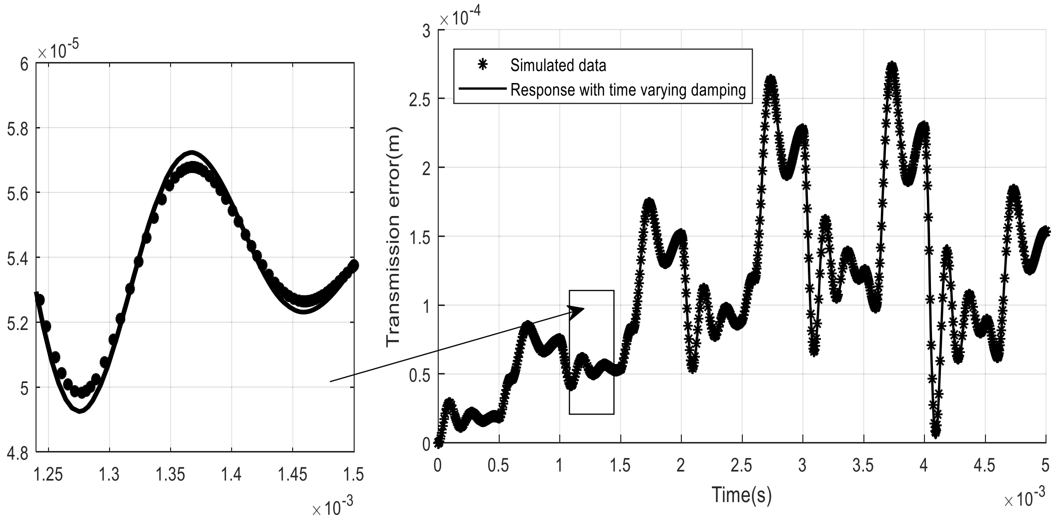

Figure 9. Identified time-varying damping modeled response versus observed response of spur pair-gear system.

captures the decrease after 0.000124 s but the peaks are underestimated. So, the varying model can be used to capture the realistic damping in the system.

4.3. *Identification of damping ratio of a gear system using CWT*

The CWT method can be used to validate the constant damping model using the damping ratio in each frequency. Firstly, the simulated data is presented in the time-frequency domain using the CWT. Figure 10 shows the wavelet demodulation plot. From the spectrum plot presented in Figure 11, frequency and damping ratio corresponding to each mode can be identified: the first frequency is localized at 1731 HZ, the second frequency neighbors 7375 HZ and the third frequency neighbors 14,750 HZ. Then, the envelope detection technique was applied independently for each frequency.

Using the wavelet envelope, the dominant frequency is localised in the second frequency. The damping ratio is not constant. It is about 0.0438 near the first frequency and then decreases to about 0.1410. However, the second frequency presents a maximum damping ratio value of about 0.1410, which is very close to the damping ratio estimated using the integral method $\xi_{\text{integral method}} = 0.09$ which can be calculated using (18)

$$\xi_{\text{integral method}} = \frac{C_{\text{integral method}}}{2 \times w_0} \tag{18}$$

where w_0 is the natural frequency and the damping value given by

$$w_0 = \sqrt{\frac{\text{mean}(k(t))}{M_e}} \tag{19}$$

$$C_{\text{integral method}} = 1.76 \times 10^4 \text{ kg}\cdot\text{s}^{-1}. \tag{20}$$

The wavelet demodulation method is usually used in the prediction of damping model in the vibrational system from a simulated response. However, based on the previous results, the constant damping obtained, through the CWT method, is insufficient as it fails to predict the simulated response in comparison to the time-varying model obtained using the integral method.

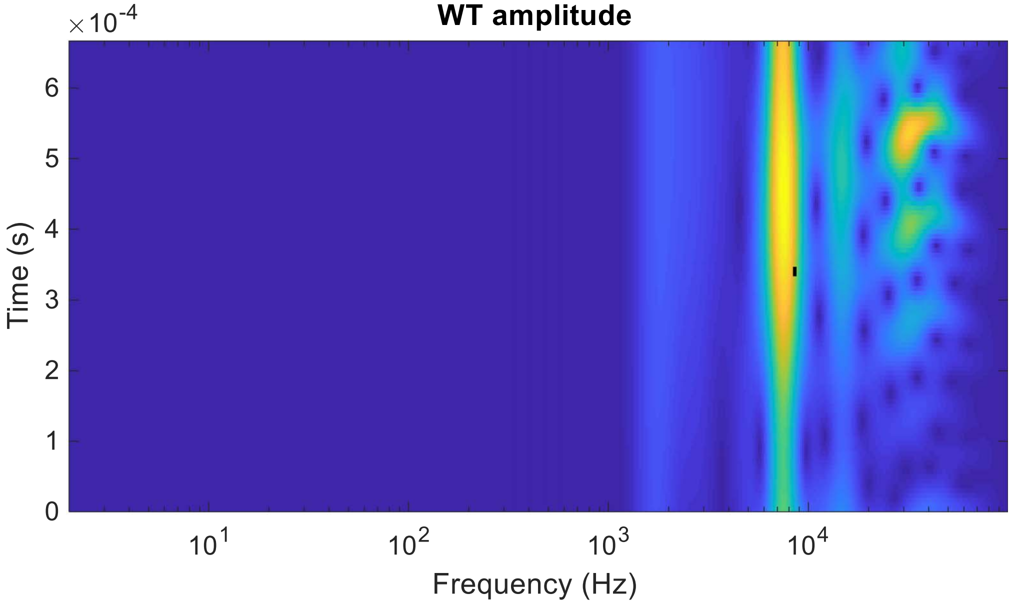

Figure 10. Wavelet plot of the simulated data.

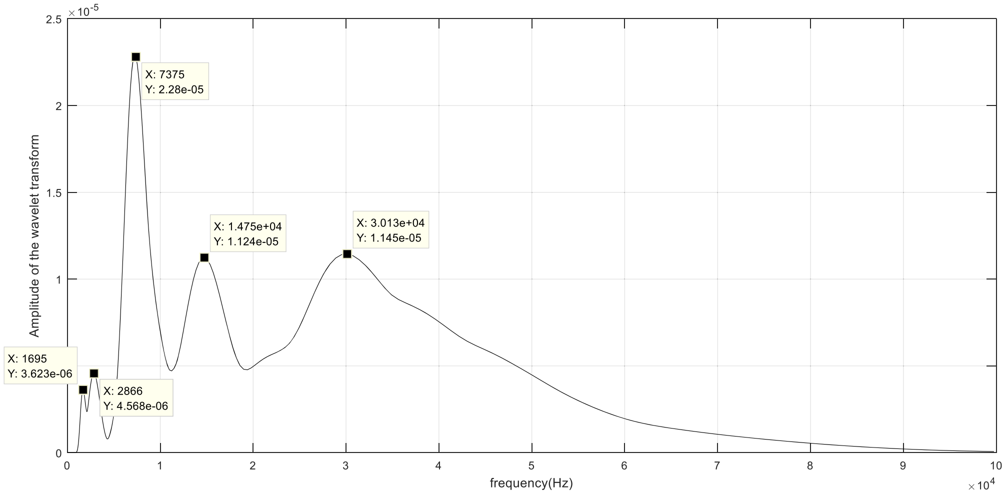

Figure 11. The power spectrum of the simulated response.

Table 2. Frequency and damping ratios using wavelet transform

Parameter	1	2	3	4
Frequency (Hz)	1731	7375	14,750	3000
Damping ratio (%)	0.0438	0.1410	0.032	0.0277

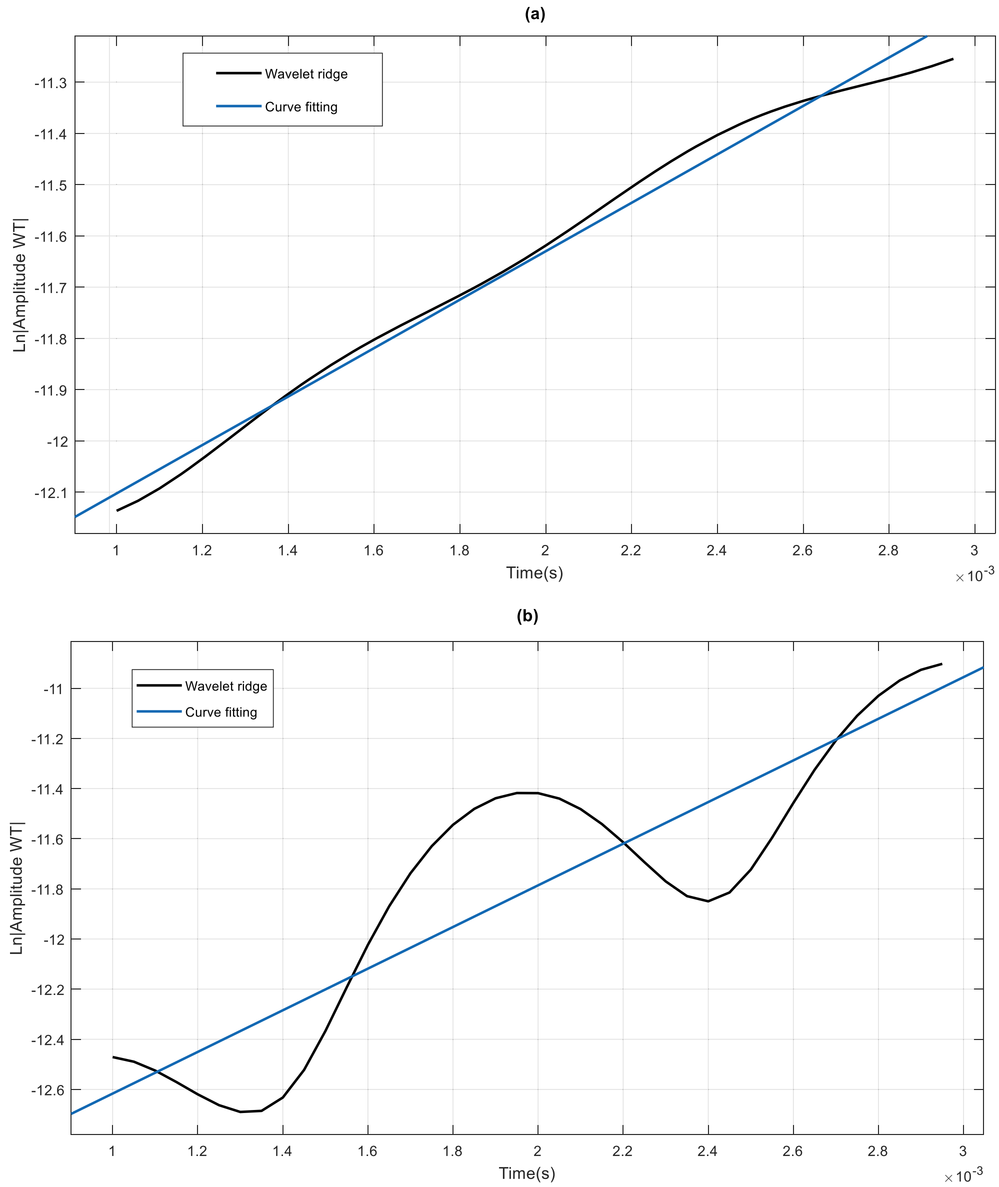

Figure 12. (a) Semi-logarithmic plot of the envelope versus the best-fit curve at the second frequency. (b) Semi-logarithmic plot of the envelope versus the best-fit curve at the fourth frequency.

5. Conclusion

In this paper, a new formulation of the integral method from a simulated response of second-order systems with time-varying load is presented. In order to predict response, a strong modification in the current integral method presented in [13] must be added. So, all matrix and vectors are reformulated. The technique can be started by a constant model damping, and then a time-varying model is presented. Then, the limits of the current integral method are presented. Simulated data is used to validate the proposed algorithm.

From the obtained results, we proved that the damping ratio depends on the time-varying load. It can be observed that the current integral method fails to identify the damping model and proves the concept of the new formulation proposed in this research. Finally, our study is very crucial for modeling, especially for parameter identification tasks.

In future investigations, integral method will be used to identify the damping model of a two-stage gear system and detect the weak nonlinearities on damping.

Conflicts of interest

Authors have no conflicts of interest to declare.

References

[1] R. B. Randall, "A new method of modelling gear faults", *J. Mech. Des.* **104** (1982), p. 259-267.

[2] F. Chaari, W. Bartelmus, R. Zimroz, T. Fakhfakh, M. Haddar, "Effect of load shape in cyclic load variation on dynamic behavior of spur gear system", *Key Eng. Mater.* **518** (2012), p. 119-126.

[3] W. Guangjiana, C. Lina, Y. Lia, Z. Shuaidonga, "Research on the dynamic transmission error of a spur gear pair with eccentricities by finite element method", *Mech. Mach. Theory* **109** (2017), p. 1-13.

[4] E. Rocca, R. Russo, "Theoretical and experimental investigation into the influence of the periodic backlash fluctuations on the gear rattle", *J. Sound Vib.* **330** (2011), p. 4738-4752.

[5] A. Hammami, A. Fernandez Del Rincon, F. Chaari, M. Iglesias, "Effects of variable loading conditions on the dynamic behaviour of planetary gear with power recirculation", *Measurement* **94** (2016), p. 306-315.

[6] F. H. Liu, S. Theodossiades, L. A. Bergman, A. F. Vakakis, D. M. McFarland, "Analytical characterization of damping in gear teeth dynamics under hydrodynamic conditions", *Mech. Mach. Theory* **94** (2015), p. 141-147.

[7] J. W. S. Rayleigh, *Theory of Sound*, 2nd ed., vol. 2, Dover Publications, New York, 1877 (1945 reissue).

[8] Y. M. A. Hashash, D. Park, "Viscous damping formulation and high frequency motion propagation in non-linear site response analysis Park", *Soil Dyn. Earthq. Eng.* **22** (2002), p. 611-624.

[9] N. Yousfi, B. Zghal, A. Akrout, L. Walha, M. Haddar, "Selection of viscous damping coefficients using the continuous wavelet transform method for a gear system", *J. Theor. Appl. Mech.* **58** (2020), no. 3, p. 585-598.

[10] M. Amabili, A. Rivola, "Dynamic analysis of spur gear pairs: steady-state response and stability of the sdof model with time-varying meshing damping", *Mech. Syst. Signal Process* **11** (1997), no. 3, p. 375-390.

[11] R. Guilbault, S. Lalonde, M. Thomas, "Nonlinear damping calculation in cylindrical gear dynamic modeling", *J. Sound Vib.* **331** (2012), no. 9, p. 2110-2128.

[12] S. Li, A. Kahraman, "A spur gear mesh interface damping model based on elastohydrodynamic contact behaviour", *Int. J. Powertrains* **1** (2011), no. 1, p. 4-21.

[13] N. Yousfi, B. Zghal, A. Akrout, L. Walha, M. Haddar, "Damping models identification of a spur gear pair", *Mech. Mach. Theory* **122** (2018), p. 371-388.

[14] L. Walha, T. Fakhfakh, M. Haddar, "Nonlinear dynamics of a two-stage gear system with mesh stiffness fluctuation, bearing flexibility and backlash", *Mech. Mach. Theory* **44** (2009), p. 1058-1069.

[15] N. Wongvanich, C. E. Hann, H. R. Sirisena, "Minimal modeling methodology to characterize non-linear damping in an electromechanical system", *Math. Comput. Simul.* **117** (2015), p. 117-140.

[16] C. Hann, M. Snowdon, A. Rao, O. Winn, N. Wongvanich, X. Chen, "Minimal modelling approach to describe turbulent rocket roll dynamics in a vertical wind tunnel", *Proc. Inst. Mech. Eng. G J. Aerosp. Eng.* **226** (2011), p. 1042-1060.

[17] C. E. Hann, J. Chase, J. Lin, T. Lotz, C. Doran, G. Shaw, "Integral-based parameter identification for long-term dynamic verification of a glucose-insulin system model", *Comput. Meth. Programs Biomed.* **77** (2005), p. 259-270.